INTEGRATED STUDY OF OPTICAL-METEOROLOGICAL PARAMETERS OF THE ATMOSPHERE NEAR COLIMA VOLCANO (MEXICO) PART I. DRY SEASON

L.S. Ivlev, V.I. Kudryashov, M.E. Arias, and O.A. Vargas

Scientific Research Institute of Physics at Sankt-Petersburg State University, Russia
Center for Atmospheric Studies at University of Colima, Mexico
Received May 5, 1997

Results of integrated experiment on determination of optical and meteorological parameters of lower atmospheric layers, performed prior, during, and after eruptions of Fuego de Colima and Popocatepetl volcanoes in dry season of 1994–1995 are presented. We measured atmospheric aerosol optical depths, atmospheric transmittances, diurnal variations of ozone concentration and concentration of aerosol particles in size range from 0.4 *to over* 10 mm. *The multielement composition of aerosol and its change with time are determined for different observation sites, and the results are analyzed with regard for existing meteorological conditions.*

1. INTRODUCTION

The part of powerful volcanic eruptions in global change of atmospheric radiative characteristics and, consequently, in weather and climate change has been well established recently.[1–5] However, very few papers have discussed influence of weak continuous emissions of volcanic substance on optical-meteorological parameters of the atmosphere in regions with active volcanoes, such as Mexico. These volcanoes inject into troposphere many solid particles of both magmatic and soil origins, sulfur gases, water vapor, etc., that exert weaker influence on the composition and physical-chemical properties of the troposphere.

These volcanic products are responsible for formation of finely dispersed sulfur-acid and sulfate aerosol particles in the troposphere, and, partly, for gain and loss of tropospheric ozone molecules. Besides, the increased concentration of sulfur gas results in additional absorption of UV solar radiation in the troposphere.

Hygroscopic particles emitted into the troposphere by volcanoes act to intensify cloud formation and, possibly, precipitation processes. The strength of volcanic effect on optical-meteorological parameters of the lower atmospheric levels is determined by both the rate of volcanic emissions and location of an active volcano. From this viewpoint, Mexico represents an ideal region for study of the influence of volcanic activity on composition and radiative characteristics of the troposphere.

2. MEASUREMENT SITE LOCATION AND INSTRUMENTATION USED

The integrated measurements of atmospheric characteristics were performed near Fuego de Colima volcano during the period from December of 1994 to October of 1995 in the dry and wet seasons. We used the data of automatic meteorological stations located at Volcancito and at the Center for Atmospheric Studies, University of Colima. The first station is located in the immediate vicinity of the crater of Fuego de Colima volcano at height 3500 m above the sea level, and the second one is in the northern part of Colima-city at height 500 m above the sea level and 40 km away from the volcano. Such location of stations allows detailed study of mountain-valley circulation and vertical stratification of temperature and humidity fields.

UV radiation measurements were performed near rancho Refuhio, 1500 m above the sea level and 15 km away from Fuego de Colima volcano. Measurements of total and diffuse radiation were made using standard actinometric instruments: UV Epply radiometers operating in the wavelength range 290–385 nm. Using standard methods,[6,7] from total and diffuse radiation measurements we calculated total and residual atmospheric optical depths τ_t and τ_a, as well as atmospheric transmittance q.

The residual atmospheric optical depth is usually assumed to be aerosol, what is not generally correct in the UV spectral range, where this characteristic may contain significant contribution from attenuation by water vapor, ozone, and sulfur gas molecules. The atmospheric aerosol optical depth characterizes quite accurately the total aerosol content of the atmosphere, and, under certain *a priori* assumptions on aerosol microstructure, the aerosol mass concentration (in g/m^2) in the entire atmospheric depth can be readily calculated from it.

In the near-ground aerosol layer, we measured aerosol concentration and size spectrum of particles in size range $0.4 < d < 20$ μm using the photoelectric

0235-6880/98/07 645-18 $02.00

particle counter A3–5M, size spectrum and morphological structure of aerosol particles in size range $0.01 < d < 20$ μm using two-cascade impactor of NIIF LGU–1982 series,[8] chemical and multielement composition of aerosols using filter sampler with one- and three-cascade filters made of FP material,[9] and concentrations of sulfur dioxide, ammonium dioxide, and ozone. Measurements of these gaseous admixtures were performed using hemiluminescent gas analyzers designed by AO "OptekB[10]

Our main goal was to study the behavior of volcano-emitted aerosols in the lower atmospheric layers and, in particular, the interaction of meteorological characteristics and concentrations of reactive gaseous species with aerosols; so most interesting to us was to estimate the influence of emissions from Fuego de Colima volcano on atmospheric characteristics in its vicinity. From this viewpoint, the entire measurement period in dry season should be divided into two parts: December of 1994, prior to the eruption of Popocatepetl volcano, and January-June of 1995, when the influence of products emitted by this volcano became significant in the lower layers of the atmosphere.

3. MEASUREMENTS IN DECEMBER 1994

3.1. Meteorological observations

In December of 1994, there was quite stable circulation of air masses in the vicinity of Fuego de Colima volcano. Around Volcancito, the direction of air flow was approximately 135°±45° (Fig. 1*a*), with strong changes in wind direction recorded only during afternoon hours. Diurnally, wind changed direction markedly and regularly on December 10–11, when it veered from 150° at nighttime and morning hours to 50° at evening-nighttime hours, and back to 150° at afternoon hours on December 11; similar behavior was observed on December 17–18; on December 19, wind changed from 100° at nighttime-morning hours to 320° in the evening. In the region of University center, every day we observed distinct change in wind direction from 30° ± 25° at nighttime-morning hours to the opposite direction between 08:00 and 12:00 LT, with subsequent recovery between 20:00 and 24:00 LT. Strongest variations in wind direction were observed in the morning hours, between 07:00 and 12:00 LT. In Volcancito, the horizontal speed of air flows varied between 1 and 8 m/s, somewhat weakening to 1–6 m/s during afternoon hours between 12:00 and 20:00 LT.

In diurnal behavior of wind speed, there were frequently observed bimodal and even trimodal distributions: most distinct maximum was recorded between 19:00 and 22:00 LT, while the single-peak pattern between 00:00 and 12:00 LT frequently broke down into two peaks at 01:00-04:00 LT and 09:00–12:00 LT (Fig. 1*b*). The inverse pattern was observed for the near-ground layer of Colima-city: the wind speed practically remained unchanged about 1 m/s between 20:00 and 11:00 LT and subsequently increased to 2–3 m/s during afternoon hours between 12:00 and 19:00 LT. At nighttime hours, approximately between 02:00 and 04:00 LT, weak secondary maximum of wind speed of 1.5–2 m/s was frequently observed (Fig. 1*c*).

The diurnal temperature behavior at both observation sites was driven by insolation regime, and was quite stable during a day (Figs. 2*a* and *c*). Between December 10 and 25, the diurnal temperature variations ranged from 4 to 11°C for Volcancito, and from 20 to 32°C for Colima-city. For Volcancito, the range of temperature variations on different days was more significant, particularly at daytime hours, when almost identical patterns of diurnal temperature variations were observed for the city, with lowest temperatures (19–21°C) at 07:00 LT and highest temperatures (28.5–32.5°C) between 12:00 and 16:00 LT. Diurnal temperature variations, somewhat atypical for Volcancito, were observed on December 18 and 19, when between 11:00 and 13:00 LT there was recorded a small temperature drop due to increase in cloud amount and subsequent precipitation.

The diurnal behaviors of relative humidity at Volcancito and Colima-city strongly differ (Figs. 2*b* and *d*). At Volcancito, for the upper limit of recorded relative humidity, the diurnal variations are practically absent, and the relative humidity is close to the saturation level; for the lower limit, the relative humidity has two peaks, one between 02:00 LT and 09:00 LT and the other between 12:00 LT and 18:00 LT. Most probable values of relative humidity are about 70±10%, what favors condensational growth of aerosol particles, primarily hygroscopic-type (sulfate- and sulfuric-acid-bearing) particles. Interestingly, at noon of December 18, precipitation was observed in the atmosphere, seemingly initiated by the presence of many hygroscopic particles of volcanic origin. In the near-ground layer of urban air, there is distinctly high relative humidity of 85±10% between 20:00 LT and 08:00 LT, and low relative humidity less than 70% between 10:00 LT and 16:00 LT, probably because of convective lifting of moist air to the higher atmospheric layers, and the return sinking of dryer air from those layers.

Thus we can conclude the following.

(1) In December, quite stable meteorological situation has been reached in vicinity of Colima volcano.

(2) In Colima-city, conditions arose which favored accumulation of atmospheric pollution in the evening, overnight, and in the morning.

(3) At night, the air masses descended from the summit of Colima volcano downward to the town.

(4) Favorable conditions were realized for condensational growth of aerosol particles, during almost entire day – in the troposphere, and during period from 20:00 to 08:00 LT – in the near-ground atmospheric layer.

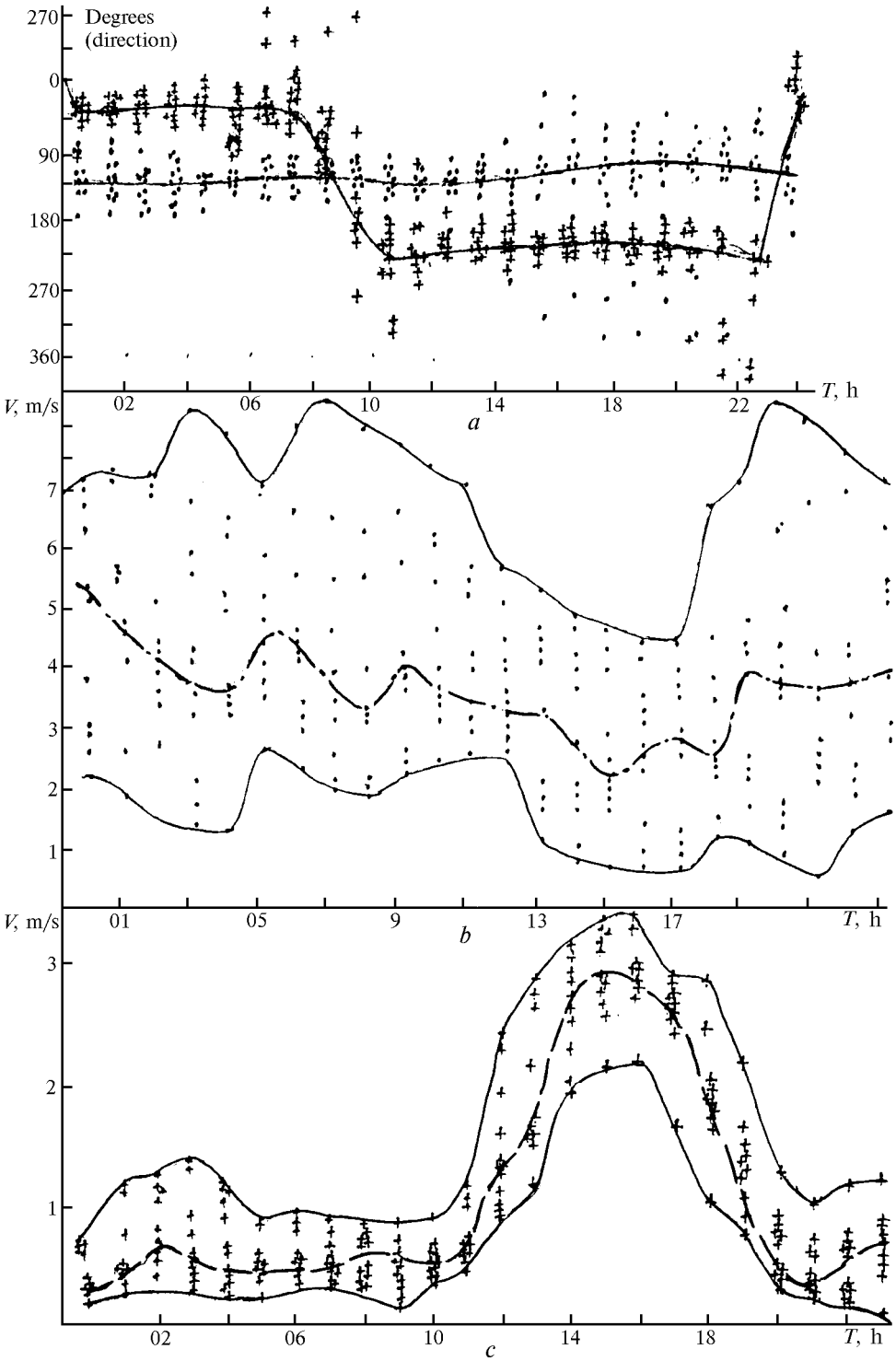

FIG. 1. Diurnally mean variations of wind direction (a) and wind speed (b) for two observation sites: the University Center for Atmospheric Studies, suburb of Colima-city (crosses); Volcancito, 3500 m *summit in the immediate vicinity of the crater of Fuego de Colima volcano (dots) for December 10–20, 1994; and wind speed variations in the near-ground atmospheric layer of Colima-city (c).*

3.2. Aerosol observations in the near-ground atmospheric layer

The main measurement cycle using photoelectric counter was carried out in the center of Colima-city. Table I presents diurnally mean variations of the function dN/dr determined from measurements performed between December 10 and 20, 1994. Diurnal behavior of aerosol constituent in the near-ground layer of Colima-city can be assessed more exactly using dV/dr and dM/dr values calculated from the same data.

TABLE I. Mean diurnal behavior of the function dN/dr *(in* $cm^{-3}mm^{-1}$*). Measurements on December 10–12, 1994 (center of Colima-city, Leandro Vaye St., 113).*

Local time of measurement, h	Mean particle size $\bar{d}$, μm											
	12.5	8.5	5.5	3.0	1.75	1.25	0.95	0.85	0.75	0.65	0.55	0.45
01	8.88E−3	1.83E−2	7.55E−2	7.02E−1	1.35E+0	9.26E+0	5.24E+1	6.59E+1	2.18E+2	6.85E+2	9.94E+2	5.66E+2
02	9.11E−3	1.48E−2	7.72E−2	6.01E−1	1.74E+0	4.27E+0	4.21E+1	7.06E+1	2.81E+2	6.66E+2	1.02E+3	6.47E+2
03	7.63E−3	1.68E−2	7.87E−2	6.23E−1	2.65E+0	8.17E+0	4.52E+1	8.76E+1	2.48E+2	6.77E+2	1.12E+3	7.30E+2
04	7.73E−3	1.48E−2	7.66E−2	1.04E+1	1.76E+0	3.92E+0	5.46E+1	7.80E+1	2.35E+2	6.66E+2	1.10E+3	8.17E=2
05	7.33E−3	1.51E−2	7.24E−2	7.42E−1	1.97E+0	4.26E+0	3.94E+1	1.02E+2	2.17E+2	6.01E+2	1.06E+3	8.53E+2
06	8.58E−3	1.81E−2	7.93E−2	7.66E−1	2.34E+0	2.46E+1	3.34E+1	6.86E+1	1.99E+2	5.44E+2	1.14E+3	1.10E+3
07	1.78E−2	3.48E−2	1.49E−1	9.60E−1	2.70E+0	9.67E+1	3.99E+1	9.26E+1	2.93E+2	6.82E+2	1.15E+3	7.47E+2
08	2.83E−2	5.78E−2	2.15E−1	1.30E+0	4.90E+0	1.89E+1	3.75E+1	1.34E+2	3.03E+2	7.14E+2	9.54E+2	5.80E+2
09	3.57E−2	6.83E−2	3.51E−1	1.56E+0	4.88E+0	1.67E+1	1.02E+2	1.78E+2	3.38E+2	9.05E+2	8.73E+2	3.81E+2
10	3.30E−2	3.97E−2	2.30E−1	2.35E+0	2.39E+0	1.67E+1	1.24E+2	2.11E+2	5.36E+2	8.37E+2	8.02E+2	3.63E+2
11	2.35E−2	3.93E−2	1.96E−1	8.60E−1	2.34E+0	1.34E+1	5.01E+1	1.80E+2	4.50E+2	7.32E+2	8.57E+2	6.87E+2
12	2.23E−2	3.10E−2	1.45E−1	7.43E−1	1.89E+0	1.57E+1	4.31E+1	9.98E+1	3.58E+2	8.74E+2	8.70E+2	4.59E+2
13	1.41E−2	4.10E−2	1.47E−1	6.11E−1	1.69E+0	5.80E+0	5.76E+1	2.00E+2	4.76E+2	7.25E+2	6.50E+2	3.04E+2
14	1.30E−2	2.76E−2	1.23E−1	6.05E−1	1.28E+0	6.19E+0	9.46E+1	2.13E+2	5.36E+2	7.54E+2	6.20E+2	2.41E+2
15	9.77E−3	2.69E−2	2.06E−1	8.64E−1	1.56E+0	7.51E+0	8.00E+1	2.25E+2	5.68E+2	8.00E+2	6.94E+2	3.24E=2
16	1.14E−2	2.38E−2	9.16E−2	6.72E−1	1.80E+0	9.35E+0	8.11E+1	2.40E+2	3.40E+2	8.55E+2	8.60E+2	4.88E+2
17	1.36E−2	2.13E−2	1.16E−1	7.52E−1	1.55E+0	4.89E+0	4.40E+1	1.02E+2	3.00E+2	8.53E+2	8.35E+2	4.96E+2
18	1.35E−2	2.67E−2	1.25E−1	9.24E−1	2.46E+0	7.57E+0	4.65E+1	9.48E+1	3.18E+2	7.47E+2	1.08E+3	5.01E+2
19	1.04E−2	2.75E−2	1.59E−1	7.37E−1	1.79E+0	6.05E+0	5.89E+1	1.29E+2	3.76E+2	8.10E+2	8.45E+2	3.84E+2
20	1.00E−2	4.76E−2	1.35E−1	1.09E+0	1.91E+0	9.04E+0	6.53E+1	9.98E+1	2.24E+2	7.22E+2	1.00E+3	9.38E+2
21	8.77E−3	2.06E−2	1.98E−1	9.42E−1	3.17E+0	7.87E+0	5.20E+1	1.03E+2	3.05E+2	9.13E+2	1.30E+3	8.89E+2
22	1.51E−2	2.13E−2	1.55E−1	1.04E+0	3.21E+0	8.68E+0	4.29E+1	1.05E+2	2.73E+2	7.56E+2	1.07E+3	7.84E+2
23	1.56E−2	3.23E−2	1.18E−1	1.05E+0	2.65E+0	8.81E+0	3.95E+1	1.08E+2	3.10E+2	7.40E+2	1.18E+3	6.49E+2
24	9.86E−3	2.24E−2	8.88E−2	1.24E+0	1.87E+0	1.18E+1	3.58E+1	8.68E+1	2.52E+2	6.67E+2	1.05E+3	7.81E+2

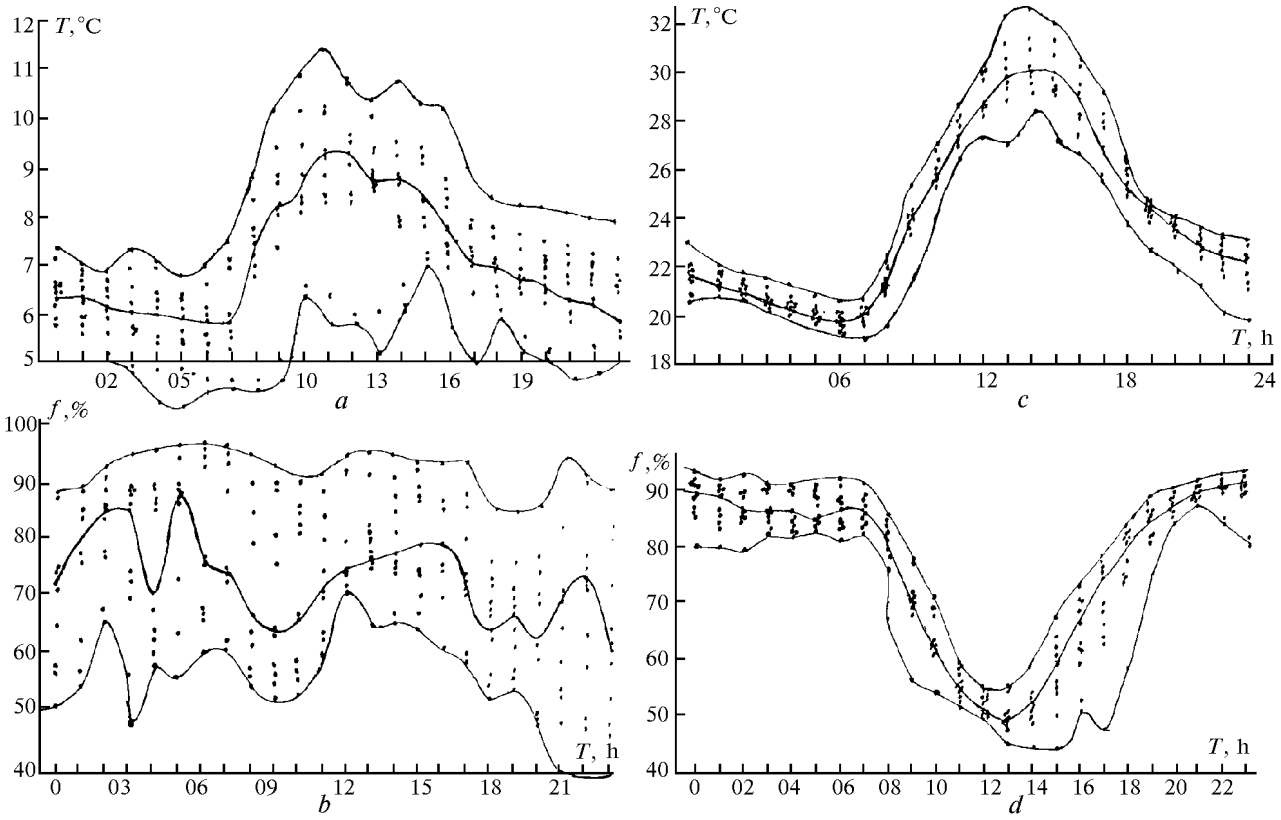

FIG. 2. Diurnal variations of temperature (a, c) and relative humidity (b, d) at two observation sites: Volcancito (a, b) and the University Center (c, d).

TABLE II. Results of multielement analysis of aerosol samples acquired in the center of Colima-city in December of 1994 (the second row contains the date of observations).

Species	Concentration, ng/m^3													Error,
	13–14	14	14–15	15	15–16	16–17	17–18	18	18–19	19	19–20	22	23	%
Al	4900	25900	1900	10100	9500	10900	8200	12900	6500	34800	9100	30400	10200	15
Si	59000	180000	17000	149000	58000	105000	113000	159000	60000	416000	115000	234000	28000	3
P	< 700	2400	< 600	2900	< 1000	700	700	< 2000	< 1000	3500	900	1500	3400	50
S	83000	120000	14000	92000	10100	148000	89000	183000	171000	181000	166000	91000	44000	20
Cl	< 70	2520	270	620	500	< 70	< 50	2120	< 100	3740	< 80	2820	3970	5
K	620	800	< 60	1040	160	1000	1070	800	230	1250	850	1550	< 200	6
Ca	2460	6410	670	5840	2030	3710	4860	5920	1570	10020	3900	7250	610	2
Ti	116	302	22	285	33	183	281	231	91	407	163	355	36	8
Cr	17	45	8	14	18	10	16	44	15	33	24	35	34	25
Mn	33	64	11	38	15	23	40	44	19	84	31	74	12	20
Fe	1130	2030	340	2130	610	1290	2200	2820	910	3430	1500	2950	300	2
Ni	7	21	4	11	10	10	9	26	14	16	13	11	20	20
Cu	17	25	3	7	24	14	19	21	26	32	19	71	86	10
Zn	28	47	4	26	26	24	32	23	13	53	33	41	24	7
Ga	1	< 3	< 1	3	2	1	< 1	8	2	4	1	3	4	40
Se	3	7	2	3	2	1	< 1	7	4	10	5	7	10	40
Br	4	11	3	5	5	5	7	10	20	13	8	11	< 6	25
Rb	5	34	3	6	14	7	2	16	< 9	23	4	7	17	30
Sr	16	19	7	18	7	14	26	37	40	53	15	37	9	25
Zr	9	26	18	15	13	10	8	21	29	19	16	18	17	30
W	< 4	< 10	< 4	5	< 6	3	4	21	42	24	5	13	29	40
Hg	< 2	< 6	< 2	6	< 4	< 2	< 1	< 6	< 6	12	4	< 4	24	15
Pb	26	61	10	42	28	33	36	48	34	58	29	46	34	10

Aerosol mass concentration substantially exceeds the maximum permissible value, especially in the morning hours. Electronic-microscopic analysis of the impactor samples indicates that most of the aerosol particles in the size range $d < 0.8$ μm are sulfate-bearing, and some of them are sulfuric-acid particles, both typically having a solid core. Multielement analysis of aerosol samples was performed using the Petryanov filters, and the results are summarized in Table II. The multielement analysis results on mass concentration and the data of photoelectric counter are in good agreement.

Using multielement analysis results, enrichment factor with respect to the earth crust composition was calculated for different species. From the diurnal behavior of enrichment factor (Fig. 3), it can be concluded that all the species can be divided into at least three groups according to their source: (a) S, Hg, Se, Cu, Ni, Rb, Ga, and Cr; (b) Br, Y, and Cl; and (c) P, Pb, Al, Zn, Fe, K, Ti, Ca, Mn, and Sr.

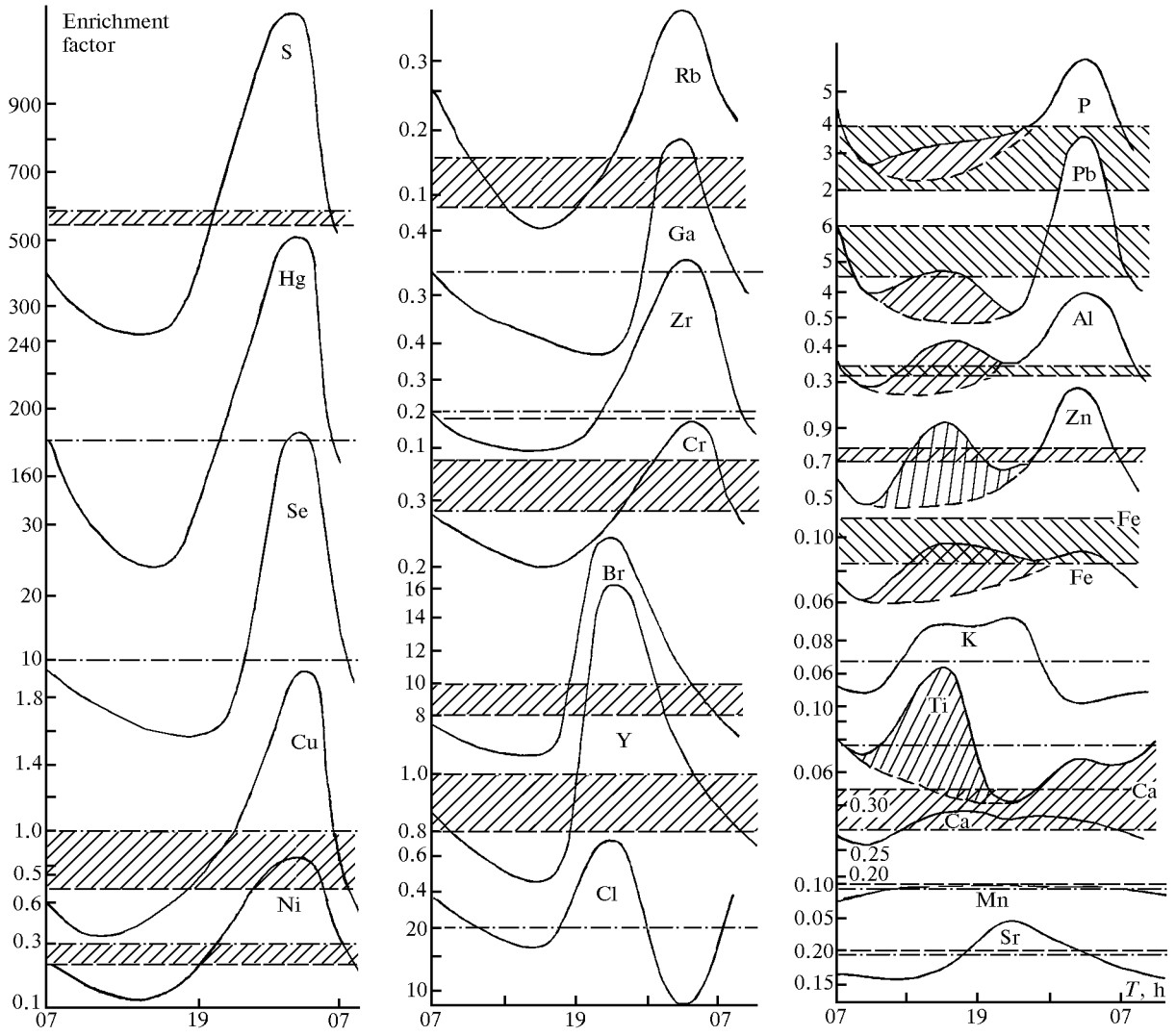

FIG. 3. Diurnal behavior of enrichment factors for different species in aerosol samples acquired in the center of Colima-city (Leandro Vaye St.) between December 10 and 20, 1994: mean enrichment factor (dot-and-dash curve), and mean enrichment factor from aerosol samples acquired at the University Center in January of 1995 (dashed line).

The species in the first group evidently are emitted by Fuego de Colima volcano; while the second group species are likely produced by the same volcano, but, perhaps, by its another part. It is less likely that for species of the first and second groups the processes of aerosol formation strongly differ. The third group species are emitted by several sources, among which possibly are soil, volcano, industry, and traffic of Colima-city. The species P, Pb, Al, Zn, and Fe exhibit morning maxima; therefore they are emitted by volcano. The chemical element K seems to belong to the second group of species. As crude estimates show, most aerosol substance, even at the center of Colima-city, is of volcanic origin.

3.3. Radiation measurements of atmospheric optical depths

The above results are supported by radiation measurements: increased atmospheric optical depths were recorded near rancho Refuhio after December 10. However, the atmospheric optical depth increased quite slowly, as aerosol substance of volcanic origin accumulated in the troposphere. On December 10, $\tau_a \approx 0$ at 09:00 LT, and it increased to 0.2–0.23 at afternoon hours; later the sky was overcast by clouds. On December 11, the residual optical depth has increased to 1.0–1.2 and rapidly became even larger once clouds appeared. Possibly, the latter effectively scavenged the atmosphere, so that during December 12 and 13, the residual optical depth markedly decreased to $\tau_a = 0.25$ and even to $\tau_a = 0.15$ (on December 13 at 11:00 LT). Subsequently, the atmospheric optical depth steadily grew until December 18 to a maximum aerosol optical depth $\tau_a = 1.60$–1.80. Then, the residual atmospheric optical depth again decreased to $\tau_a < 0.1$. On these decline days, the measured optical depth τ_a exhibited strong abrupt increases to $\tau_a = 1.3$–5.0 and relatively blurred increases lasting 20–40 min (Fig. 4). The latter took place when cirrus clouds appeared.

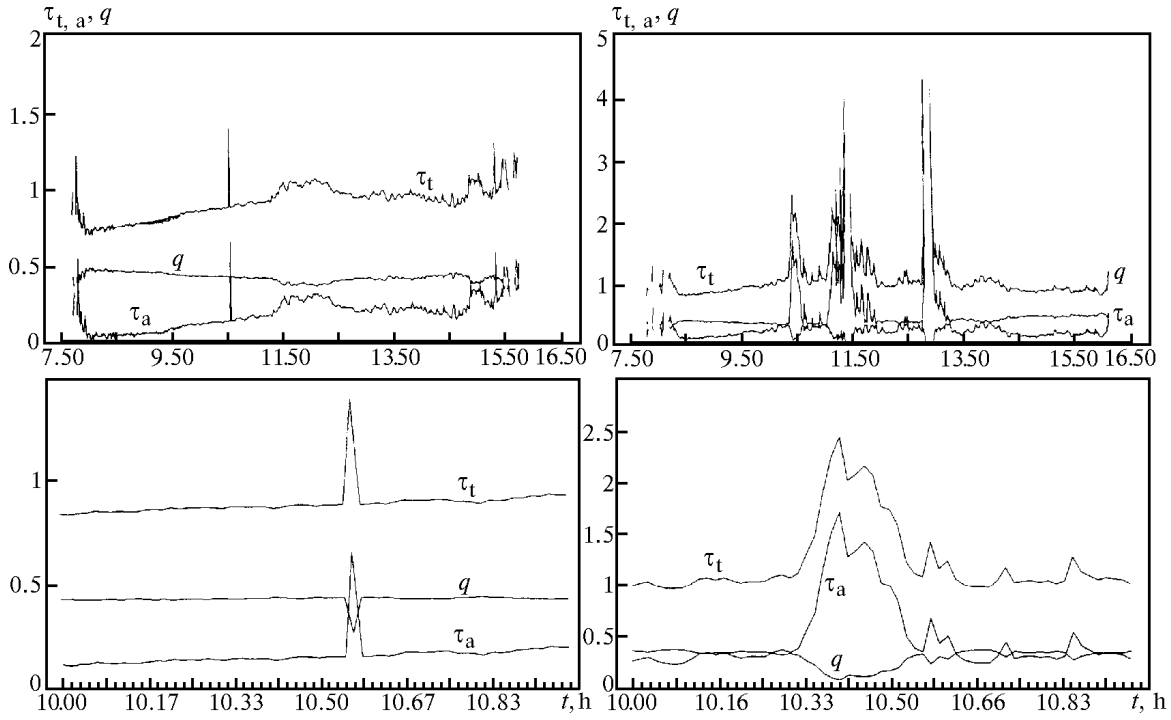

FIG. 4. Two types of fluctuations of atmospheric optical characteristics (τ_t, τ_a, q) (top row): December 13 (left) and December 19 (right). Time variations of τ_t, τ_a, and q in another time scale (bottom row).

In the first case, the clouds could not be visually identified. Probably, such events are caused by the appearance of cloud structures with very small particles ($d \le 0.3$ μm) in the atmosphere, which perhaps not only scatter, but also absorb radiation in the UV spectral range.

3.4. Discussion of measurement results obtained in December of 1994

When compared directly, the microscopic and optical measurement results do not totally agree, though both indicate that first the aerosol substance accumulates, and then the atmosphere is scavenged. The explanation that the microphysical measurements provide data on aerosol content in the near-ground layer only, while optical measurements pertain to the entire atmospheric depth, is not convincing, because most aerosol substance resides in the near-ground layer, and, in addition, mixing of impurities occurs during a day, both in the near-ground and higher atmospheric layers. More likely, the reason might be due to the variability of size distribution function of aerosol particles, which, in turn, affects strongly the aerosol optical properties.

In the initial stage of the study, the data were insufficient to calculate aerosol optical properties correctly; so only specific surface area of aerosol particles was calculated from data of photoelectric counter.

Figure 5 presents the calculation results on time variations of mass concentration m_a of aerosol particles, specific surface area S_a of aerosol particles in size range $0.5 \le d \le 0.7$ μm, and τ_a measured between 11:00 and

12:00 LT, when marked vertical mixing of atmospheric layers takes place. It is evident that m_a and τ_a do not correlate, while τ_a and S_a curves ($0.5 \le d \le 0.7$) match closely.

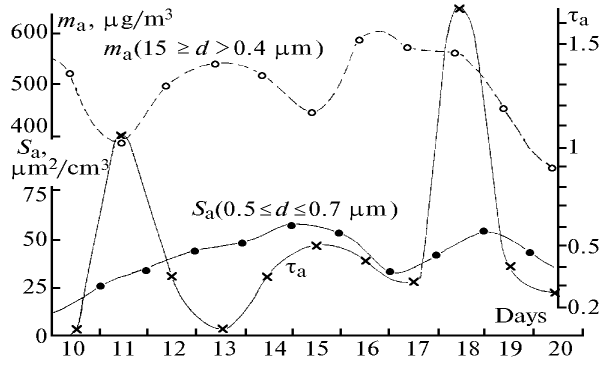

FIG. 5. Time behavior of different aerosol characteristics at rancho Refuhio in the period from December 10 to 20, 1994. Here, τ_a is the atmospheric aerosol optical depth in the UV spectral range.

This suggests that the giant particles, although prevailing in the near-ground atmospheric layer, contribute little to the extinction of solar radiation, and that the giant and small particles evolve in the opposite directions: gain in the giant particles means the loss in the small ones in size range $0.5 \le d \le 0.7$ μm and vice versa. Such diverse behavior of different-sized particles is possibly due to specific features of volcanic emissions and existence of processes of aerosol particle formation from volcanic gases.

The particles formed by volcano serve as condensation nuclei in cloud formation, that explains increases in cloudiness after volcanic emissions. The formed cloudiness, in its turn, acts as volcanic aerosol scavenging mechanism in the troposphere, what was the case on December 18, when precipitation fell near Fuego de Colima volcano.

4. EXPERIMENTAL STUDIES IN JANUARY-JUNE, 1995

4.1. Combined measurements of aerosol characteristics and concentration of near-ground ozone and sulfur gas

In the dry period from January to June of 1995, we performed combined measurements of aerosol characteristics and concentrations of ozone and sulfur gas in the near-ground atmospheric layer at the University Center for Atmospheric Studies. From photoelectric counter measurements, we revealed very high instability of measured aerosol characteristics, high concentration of aerosol particles with $d > 2.0$ μm in the near-ground atmospheric layer, and many cases where particle size distribution functions with very distinct maxima were found. In such cases, more than 50% of particles were sampled in just one or two measurement channels, that is in size range $\Delta d = 0.1–0.2$ μm.

The mean diurnal behavior of the parameter dV/dr is presented in Tables III and IV for the periods January–February and April–May. Characteristic of January–February measurements was the presence of three distinct maxima in diurnal variations of particle concentration:

morning maximum between 06:00 and 08:00 LT for particles with $d \ge 0.7$ μm;

daytime maximum between 11:00 and 15:00 LT for particles with $d > 1.0$ μm;

evening maximum between 21:00 and 23:00 LT for particles with $10 > d > 2.0$ μm and $d < 0.7$ μm.

TABLE III. Diurnal variations of the function dV/dr for January-February of 1995 in the suburb of Colima-city (CUICA).

$\bar{d}$, μm	Local time, h											
	01	02	03	04	05	06	07	08	09	10	11	12
12.5	14.6	13.2	11.8	11.3	10.8	12.6	14.3	14.1	13.9	11.2	8.61	8.88
8.5	5.90	5.62	5.34	6.39	7.42	9.91	12.4	11.5	10.7	8.82	6.98	7.28
5.5	4.95	5.31	5.67	13.4	21.2	18.3	15.4	15.1	14.8	11.3	7.75	6.91
3.0	8.22	10.2	12.2	14.0	15.7	19.4	23.2	20.6	18.0	13.2	8.46	8.08
1.75	4.07	4.02	3.97	5.76	7.56	10.7	13.9	12.6	11.4	6.64	1.92	3.10
1.25	4.91	6.80	8.70	10.7	12.7	15.2	17.7	17.2	16.7	8.98	1.23	1.79
0.95	9.78	17.4	25.0	42.4	59.8	71.8	83.7	80.9	78.2	43.3	8.48	14.4
0.85	23.1	37.4	51.7	62.4	73.0	92.8	112.6	113.3	114.0	73.6	33.2	38.3
0.75	34.2	46.6	59.0	79.5	90.0	95.9	101.8	98.0	94.2	73.2	52.3	64.8
0.65	47.5	43.6	39.8	40.6	41.5	38.4	35.2	35.3	35.4	48.9	62.4	68.9
0.55	53.6	42.7	31.8	24.5	17.2	13.2	9.12	22.3	35.4	48.9	62.4	68.9
0.47	2.10	1.80	1.50	1.95	2.40	2.95	3.50	2.92	2.35	7.74	13.14	11.35

$\bar{d}$, μm	Local time, h											
	13	14	15	16	17	18	19	20	21	22	23	24
12.5	9.14	9.56	9.97	9.82	9.67	8.54	7.42	7.80	7.96	7.62	7.29	10.9
8.5	7.59	8.60	9.62	9.50	9.37	7.08	4.79	17.2	22.4	21.0	19.6	12.6
5.5	6.07	9.30	12.5	9.80	7.07	8.00	8.93	11.1	13.3	12.2	11.0	7.98
3.0	7.70	9.06	10.4	8.76	7.11	6.92	6.73	8.05	9.24	9.54	9.84	9.03
1.75	4.28	5.20	6.13	4.72	3.30	2.56	1.82	3.20	4.42	5.51	6.60	5.34
1.25	2.36	5.34	8.22	7.52	6.71	4.00	1.28	1.12	0.46	0.58	0.70	2.80
0.95	20.3	27.7	35.0	46.3	47.5	25.3	3.18	9.20	14.9	12.8	10.8	10.28
0.85	43.3	61.9	80.5	101.7	122.9	68.9	15.0	11.5	7.90	13.7	19.4	31.4
0.75	77.2	66.1	55.5	83.9	112.7	69.8	26.8	22.4	18.0	28.4	38.9	57.2
0.65	75.5	77.5	79.4	68.2	57.0	50.1	43.2	44.4	45.6	53.8	62.0	68.7
0.55	75.5	54.1	32.7	21.5	10.3	26.8	43.3	44.0	43.9	46.7	49.5	62.5
0.47	9.56	8.12	6.67	4.60	2.53	13.1	23.7	16.2	56.0	30.5	0.50	5.03

TABLE IV. Diurnal variations of the function dV/dr *for April–June of 1995 at the University Center (CUICA).*

$\bar{d}$, μm	Local time, h											
	01	02	03	04	05	06	07	08	09	10	11	12
12.5	6.60	5.89	5.18	5.01	4.84	11.2	11.1	11.0	9.68	9.68	9.68	11.2
8.5	5.18	4.01	2.84	2.53	2.22	5.06	5.12	5.18	6.66	7.03	7.40	6.90
5.5	4.25	3.96	3.67	3.45	3.23	7.11	7.81	8.51	7.11	8.40	9.68	10.0
3.0	4.31	3.90	3.50	3.58	3.65	53.2	44.7	36.2	7.79	7.15	6.51	6.46
1.75	2.04	1.98	1.92	1.74	1.56	0.54	1.57	2.60	3.72	2.19	0.66	5.98
1.25	0.911	0.808	0.704	0.704	0.704	0.400	0.652	0.704	0.726	1.23	1.74	15.9
0.95	1.78	1.88	1.98	2.40	2.83	3.73	3.74	3.79	5.75	6.32	6.90	85.4
0.85	3.26	3.44	3.61	3.60	3.58	16.0	9.30	2.60	9.92	11.4	12.9	78.6
0.75	6.51	6.82	7.1	11.1	15.0	18.9	32.1	45.3	9.92	11.4	12.9	78.6
0.65	18.2	18.9	39.8	42.4	46.0	29.2	46.4	63.6	45.3	41.8	38.2	79.9
0.55	53.6	48.7	43.8	36.0	30.2	35.6	37.3	39.1	46.8	60.2	73.5	53.6
0.47	54.2	46.2	38.3	35.6	33.0	22.0	20.4	18.3	57.4	77.4	78.0	39.0

$\bar{d}$, μm	Local time, h											
	13	14	15	16	17	18	19	20	21	22	23	24
12.5	13.8	11.0	9.24	9.90	10.6	7.70	4.84	4.40	3.96	4.02	4.09	5.34
8.5	6.41	7.77	9.13	7.90	6.66	5.62	4.69	13.6	22.4	21.6	20.8	13.0
5.5	10.4	9.86	9.31	7.37	5.43	5.43	5.43	8.40	11.4	11.7	12.0	8.14
3.0	6.42	7.19	7.96	6.56	5.17	5.66	6.14	5.95	5.76	5.75	4.74	4.52
1.75	11.3	8.46	5.64	5.59	5.54	3.90	2.26	3.49	4.72	5.66	6.60	4.42
1.25	30.1	19.3	8.51	5.55	2.59	2.38	2.16	1.56	0.955	0.698	0.440	0.676
0.95	164.0	164.0	164.0	93.2	22.7	15.4	8.10	13.0	17.8	15.3	12.7	7.24
0.85	144.0	137.0	130.0	83.0	36.2	24.5	12.9	7.88	2.90	2.66	2.43	73.4
0.75	144.0	170.0	197.0	143.0	89.2	41.2	0.163	0.810	1.45	2.48	3.52	73.9
0.65	122.0	96.6	71.1	54.5	37.9	22.8	6.69	5.87	4.65	7.23	9.81	65.7
0.55	32.7	22.6	12.6	10.9	9.23	14.8	20.3	32.1	23.9	31.2	39.5	36.1
0.47	0.00	0.10	0.20	25.6	51.1	73.0	95.0	90.3	85.6	80.3	75.6	37.5

For particles in other size ranges, the maxima were either absent or shifted in time. As compared with January–February measurements, in May there are a considerable decrease in concentration of particles in size range $4 \geq d \geq 0.6$ μm and a marked increase in the size range $d \leq 0.6$ μm; also changing is diurnal behavior of concentration with certain increase in concentration of particles with $0.6 \leq d \leq 2.0$ μm and $d > 10$ μm at afternoon hours.

We also performed multielement analysis of aerosol filter samples, including those obtained with three-layer filters; the multielement analysis results are presented in Tables V and VI. As seen, most species have much lower concentrations than in December of 1994, consistent with the photoelectric counter measurements. At the same time, of note is the considerable variability of concentrations of some elements such as S, Cl, K, Pb, and Fe.

TABLE V. Results of multielement analysis of aerosol samples acquired at the University Center in January–May of 1995.

Species	Concentration, ng/m^3							Error, %
	23.01	31.01	1.02	3.02	3.02	19–20.05	20.05	
Al	13900	14400	14100	13100	18600	1420	3940	15
Si	115000	185000	129000	180000	179000	20600	65800	3
P	< 1000	< 1000	1900	< 1000	< 1000	< 200	< 400	50
S	45000	28000	24000	38000	48000	2390	10860	20
Cl	2800	3900	2400	2600	1500	750	160	5
K	760	740	890	1160	1590	30	330	6
Ca	4010	5740	5720	6950	6480	990	3840	2
Ti	172	371	301	341	366	107	248	8
Cr	< 10	22	31	17	35	16	29	25
Mn	39	55	33	53	56	20	36	20
Fe	1540	2710	2360	2600	2780	456	1632	2
Ni	11	7	7	12	15	8	9	20
Cu	21	24	63	26	34	7	8	10
Zn	20	14	19	18	14	2	10	7
Ga	4	2	2	4	2	5	4	40
Se	6	3	2	< 2	4	3	9	40
Br	7	3	5	7	4	8	10	25
Rb	18	9	20	18	11	5	7	30
Sr	17	44	44	48	18	17	33	25
Zr	15	16	18	38	56	16	47	30
W	11	15	9	21	12	21	20	40
Hg	< 5	< 4	< 4	< 4	< 4	5	3	15
Pb	26	18	24	27	21	7	68	10
Th	< 5	< 5	< 5	< 5	< 5	6	5	20

TABLE VI. Distribution of species over three layers of the system of dispersion filters (in percent by mass) for measurements at the University Center of Colima-city.

Species	19–20.05			20.05		
	I	II	III	I	II	III
Al	86	–	14	76	8	16
Si	97	3	–	91	8	1
S	57	24	19	42	18	40
Cl	43	–	57	100	–	–
K	100	–	–	100	–	–
Ca	86	8	6	89	10	1
Ti	67	27	6	71	27	2
Cr	23	63	14	40	60	–
Mn	45	55	–	76	24	–
Fe	91	6	3	89	9	2
Ni	22	73	5	31	60	9
Cu	–	41	59	36	23	41
Zn	100	–	–	86	–	14
Ga	32	18	50	33	67	–
Se	79	–	21	39	23	38
Br	58	42	–	39	44	17
Rb	47	–	53	52	–	48
Sr	49	21	30	64	25	11
Zr	29	32	39	36	32	32
W	36	34	30	22	40	38
Hg	61	39	–	–	100	–
Pb	59	41	–	14	81	33
Th	59	41	–	28	5	67

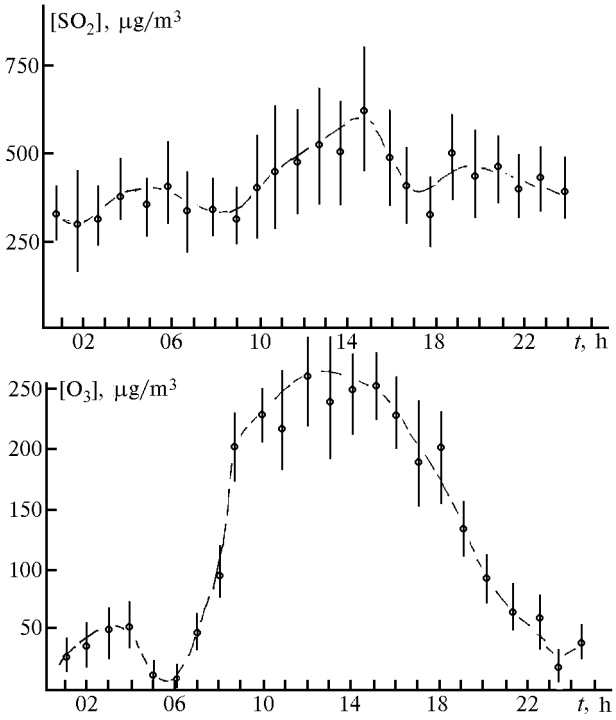

FIG. 6. Typical curves of diurnal behavior of concentration of sulfur gas $[SO_2]$ *(in* μg/m^3*) and ozone* $[O_3]$ *(in* μg/m^3*) for dry period (February of 1995) in the near-ground atmospheric layer at the University Center.*

From the data obtained with use of three-layer filters, we can conclude that some species exhibit selective character of particle size distribution functions: K, Ca, Si, Fe, and Zn have deposited almost totally on the first layer; Al, Cl, Zn, S, Se, and Rb have two-mode structure; most finely dispersed particles are those containing Th, W, Rb, Se, Cu, and S; and the Cr, Ni, Ga, Br, Hg, and Pb species have deposited on the second filter layer, what suggests their near-complete absence in the giant particles.

Measurements of diurnal behavior of ozone and sulfur gas have revealed increased concentrations of both gases, and, moreover, highly strong variability of sulfur gas concentration in the near-ground layer. The latter fact indicates the presence of powerful source of sulfur gas, whose emission rate might have strong time variations. The diurnal behavior of sulfur gas concentration is not generally well defined with frequent increased concentrations at pre-morning hours, particularly in the presence of near-ground inversions.

Typically, ozone concentration rapidly increases after sunrise. Ozone concentration normally peaks between 13:00 and 14:00 LT and sometimes even earlier. After sunset, the ozone concentration rapidly comes to zero by 22:00–23:00 LT; but during night, approximately at 03:00–04:00 LT, a weak secondary maximum of ozone concentration of 10 μg/m^3 frequently may occur (with about 30% probability). Typical curves of the diurnal behavior of concentrations of these gases are presented in Fig. 6.

4.2. Radiation measurements

Since early January of 1995, increased residual atmospheric optical depths have been observed; whereas τ_a values did not generally decreased below $\tau_a = 0.25$. A band-like structure of τ_t and τ_a was occasionally observed, evidently due to the presence of either cloud structures of fumarol type or cirrus clouds. Of most interest are cases of abrupt changes in values of τ_t and τ_a and their time behavior. These abrupt changes, typically occurring at pre-noon hours and sometimes at afternoon hours, are caused by sudden changes in wind direction, as confirmed by data of automatic meteorological stations (Table VII).

As an example, Figure 7 presents measured radiative fluxes J_{gl}, J_{dif}, and J_{dir} and calculated τ_t, τ_a, and q values for March 5, 1995. It is clearly seen that the character of behavior of these characteristics alters after 10:01 LT. Visually, we observed the appearance of a cloud structure, as a result of lifting and diffusion spreading of fumarol jet. As confirmed by data of meteorological observations, this cloud structure formed due to volcanic emission.

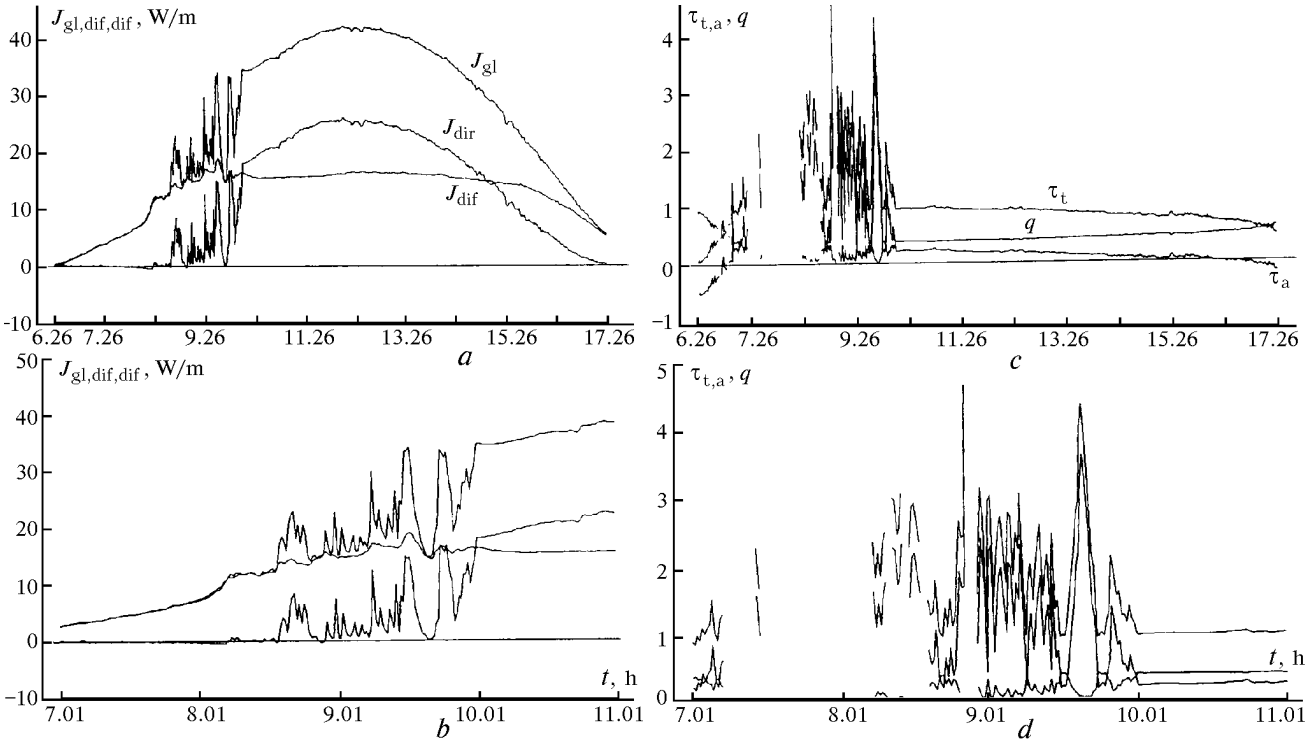

FIG. 7. Typical diurnal variations of solar radiation intensity (a, b): global J_{gl}, diffused J_{dif}, and direct J_{dir}; and the atmospheric optical depth (c, d): total τ_t and residual (aerosol) τ_a, and atmospheric transmittance q (for March 5, 1995) (top row). Time variations of J_{gl}, J_{dif}, J_{dir}, τ_t, τ_a, and q in another time scale (bottom row).

TABLE VII. Repetition rate of wind direction at different time of a day at the University Center (CUICA) and in Volcancito for March 9–10, 1995.

CUICA																									
68	9 • March • 95	1	2	3	4	5	6	7	8	9	10	11	12	13	14	15	16	17	18	19	20	21	22	23	24
0	22.5	9	8	6	6	3	5	6	9																4
22.5	45	1	3	4		3	6	2	2	3														5	6
45	67.5						1	1		2	2			1									1	7	
67.5	90																								
90	112.5									2							1								
112.5	135																1								
135	157.5									2	2	1		1											
157.5	180													1	1		1	3	2	2	4	1			
180	202.5										2	5	4	1	4	1	5	7	4	5	4	3			
202.5	225										5	4	5	5	4	6	4	1	6	4	3	6	5		
225	247.5											1		3	2	3		1		1		2	5		
247.5	270										1		1			2					1				
270	292.5											1	2		1										
292.5	315																								
315	337.5	1				2			1	3															
337.5	360	1	1	2	6	4		3	1																
69	10 • March • 95	1	2	3	4	5	6	7	8	9	10	11	12	13	14	15	16	17	18	19	20	21	22	23	24
0	22.5	5	4	6	9	11	9	7	1			1												4	4
22.5	45	6	6	6	3		3	4	4	2														7	8
45	67.5	1	2					1	6	1		1											1	1	
67.5	90								1	3	1			1											
90	112.5									4	1														
112.5	135									2					1										
135	157.5										4	2	2	1	2	1		1	2				4		
157.5	180										2			3	1	4	1	1	4	3			1		
180	202.5											1	4	1	2	3	3	6	4	6	5	4			
202.5	225										4	4	2	3	3	2	4	3	1	3	3	3	3		
225	247.5											2		2		1	2	1	1		4	2	2		
247.5	270														2	1	2					3			
270	292.5												2	1	1										
292.5	315																								
315	337.5											1											1		
337.5	360					1							2												
Volcancito																									
68	9 • March • 95	1	2	3	4	5	6	7	8	9	10	11	12	13	14	15	16	17	18	19	20	21	22	23	24
0	22.5					1	2	1			1	3					3			1	6	2	1		
22.5	45						3		2	1	1	3	1			1	2		1		4	10	1		
45	67.5						2		1	2	1		1							1	1		2		
67.5	90					1				3	4				1	2	1	1					1		
90	112.5								1	3		2	2				1	2	1				1	1	
112.5	135												2	2	1	1		4	1	2			4	2	
135	157.5			1							1	1	2	1	1	3		1	5	3			1	2	
157.5	180	10	8	4	1	2	1			1		1		1	1			3	3	3				5	3
180	202.5	2	4	4	6	3				1	1		1	3					1					2	8
202.5	225			3	4	3	1	2		1	1			2	4	3	2								1
225	247.5				1			1	2					1		1	1	1							
247.5	270					1	1	2	1								1								
270	292.5							1	1		1	1	1		1										
292.5	315							2	3			1	1		1	1									
315	337.5						1	2	1		1		1	1	1		1			1					
337.5	360					1	1	1						1	1					1	1		1		
69	10 • March • 95	1	2	3	4	5	6	7	8	9	10	11	12	13	14	15	16	17	18	19	20	21	22	23	24
0	22.5																	1	1	1					
22.5	45																		1	6	2				
45	67.5																			2	3				
67.5	90															1	2	1	2						
90	112.5									1	2		1				2	3	3						
112.5	135								1	1	4		1	2		3	2	3	5		1				
135	157.5		7	1	2					1	2	5	2	1	6	5	3	3			1			4	2
157.5	180	7	3	11	7	2	1		3	4	1	6	5	2	3	3	1								
180	202.5	5	2		3	10	11	12	8	4	3	1	2	3			1	1			1	1			
202.5	225									1			1	3	3						1				
225	247.5													1								2			
247.5	270																1				3	6	3	2	3
270	292.5																			1		2	9	6	6
292.5	315																					1			1
315	337.5																								
337.5	360																								

Figure 8 presents the data on wind direction in the regions of Volcancito and the University Center acquired on March 4 and 5; as is clearly seen, wind rapidly veers at both locations in the morning hours. In the region of Colima-city, it then comes back to the original direction (to within ±20°) at the evening hours and veers again in the morning of March 5. Unlike, in the region of Volcancito, wind veers by 70–80° during a day on March 5 and does not turn back. All these factors have led to breakdown of fumarol jet into separate pieces, in which the conversion of SO_2 into sulfuric acid and sulfates took place with subsequent growth of thus formed particles at nighttime hours (see Fig. 8). For comparison, we also present the data on atmospheric optical characteristics for March 10 (Fig. 9), the day before which no directed air flow was recorded in the region of Volcancito.

We noted a weak wind with varying direction, that prohibited formation of fumarol jet or a cloud structure of other type (see Table VII). As seen from Fig. 9, the total and residual atmospheric optical depths both slightly increase between 10:15 and 10:55 LT, the time of volcanic cloud passage over rancho Refuhio. The tropospheric air had low relative humidity; so, no condensational particle growth was observed in the cloud.

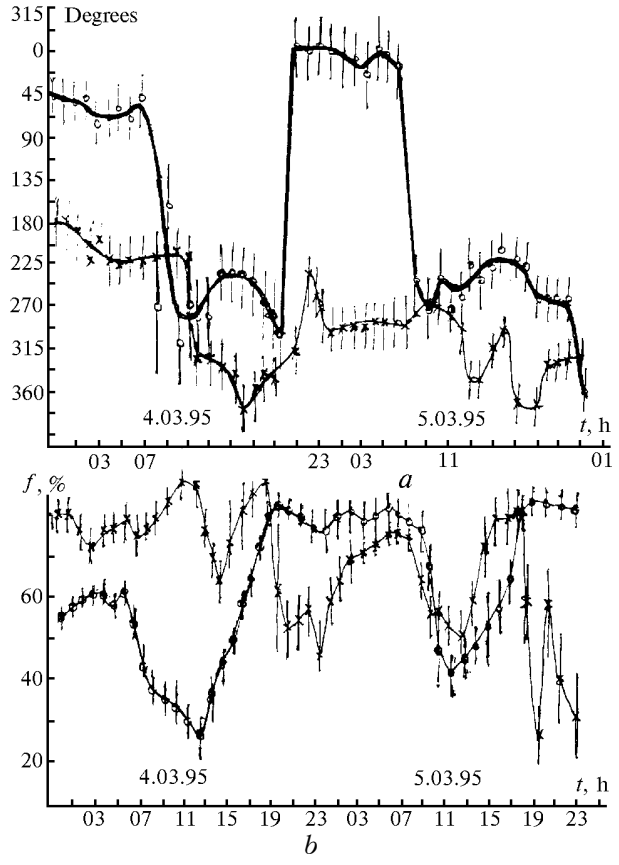

FIG. 8. Wind direction (a) and relative humidity (b) for two locations: Volcancito (crosses) and University Center (open circles) on March 4–5, 1995.

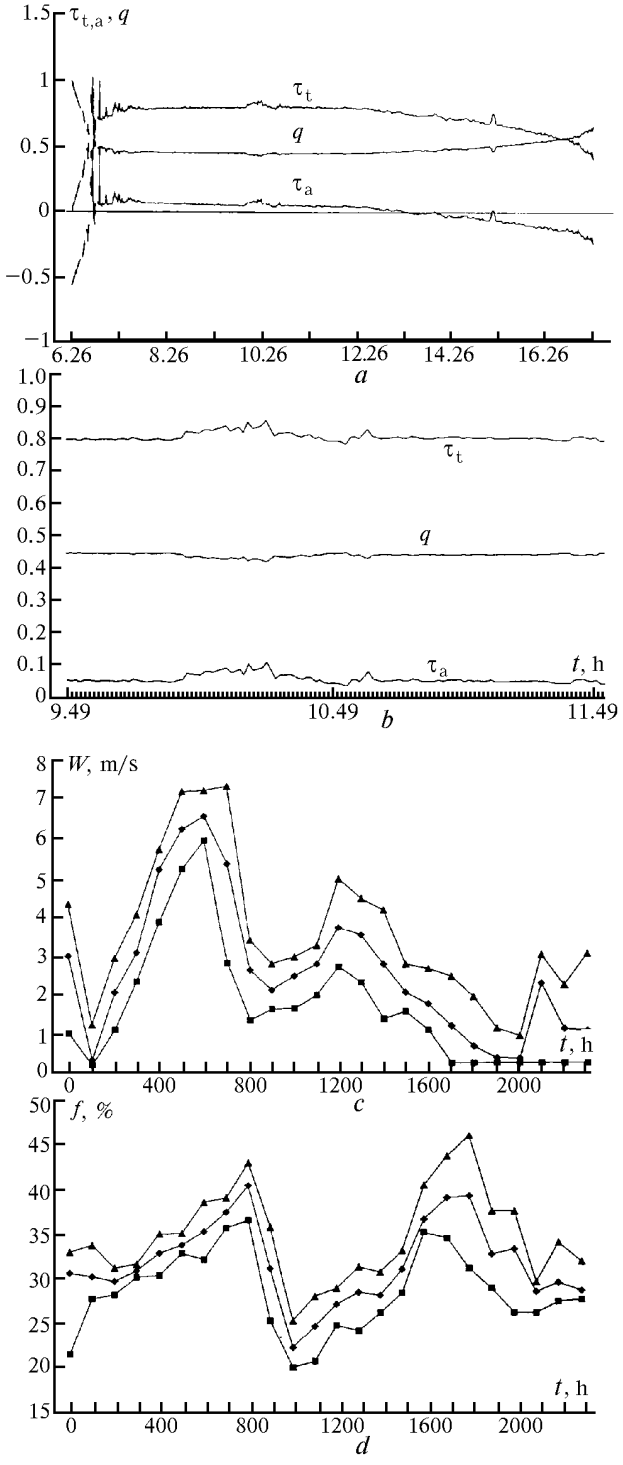

FIG. 9. Diurnal behavior of atmospheric optical parameters (a, b) τ_t, τ_a, and q (for rancho Refuhio); wind speed (c); and relative humidity (d) in Volcancito on March 9, 1995.

4.3. Integrated experiments in May of 1995

To estimate the eruption influence on atmospheric processes, of great interest was to measure atmospheric characteristics simultaneously at several locations

around the volcano. However, this was beyond our capabilities; so we performed three successive measurements at different separations from the volcano and at times quite close to one another. The first series of measurements was carried out in the region of Playon valley between Fuego de Colima and Nevada de Colima volcanoes between May 9 and 11, the second series was performed in the rancho Refuhio between May 17 and 20, and the third series was performed at the University Center for Atmospheric Studies since May 20.

4.3.1. Measurements in Playon valley

Measurements of aerosol characteristics, aerosol sampling with subsequent multielement analysis, and measurements of ozone concentration and sampling dry deposit onto polyethylene substrate all were performed in the not easily accessible region, at 3200 m height, far from the populated centers, and immediately below the crater of Fuego de Colima volcano. In the region, where measurements were conducted, there were no sources of artificial pollutants: no camp-fires were lit, and no cars approached closer than 1 km to the measurement site, so it can be considered anthropogenically unaffected.

The mean diurnal variations of aerosol characteristics obtained from photoelectric counter measurements are presented in Table VIII. On May 10, two measurements of particle size distribution, at 12:00 and 13:00 LT, were performed in the immediate vicinity of Volcancito at the height of 3400 m. In comparison with measurements at a lower height in the Playon valley, the obtained volume particle size distribution functions dV/dr have significantly higher values in the particle size range $0.5 < d < 7$ μm and much higher values in the size range $2 \geq d \geq 0.5$ μm. At nighttime hours, the lowest concentrations of giant particles were recorded. In some measurement series, the first three counter channels indicated no particles present in this size range $d \geq 4$ μm.

TABLE VIII. dV/dr *values from the measurements on May 9–11, 1995, in the region of Playon.*

$\bar{d}$, μm	Minimum	Local time, h											
		01	03	05	06	07	08	09	10	11	12	13	14
12.5	0	0.748	0.308	0.01	0	0.442	0.879	1.01	2.21	2.64	1.32	1.85	2.21
8.5	0	1.31	0.567	0.173	0	0.275	1.10	1.33	0.247	0.987	1.97	2.86	1.73
5.5	0	2.13	0.257	0.0612	0	1.68	1.39	1.42	2.49	1.39	4.11	2.17	2.49
3.0	0.101	2.66	0.770	0.101	0.129	0.330	1.47	1.98	2.64	0.572	4.03	3.30	4.64
1.75	0.016	1.38	0.498	0.048	0.0160	0.408	2.62	1.24	0.600	1.02	1.20	1.62	0.456
1.25	0.016	0.664	0.388	0.016	0.0480	0.504	2.24	1.45	1.19	1.01	1.10	1.67	0.770
0.95	0.040	2.09	0.227	0.040	0.227	1.60	5.97	2.76	2.76	4.41	0.733	1.20	2.57
0.85	0.0133	3.01	1.08	2.59	0.0133	5.28	30.3	2.69	9.09	10.2	2.31	3.45	5.44
0.75	0.0533	15.6	15.6	13.7	0.0533	12.5	46.2	17.3	19.8	8.13	9.45	2.29	12.3
0.65	10.0	39.1	26.4	37.7	10.0	44.1	99.9	41.4	84.9	146.0	37.5	15.9	25.8
0.55	29.0	52.2	43.7	44.1	41.6	64.4	86.4	79.2	77.4	48.6	43.2	39.6	57.6
0.47	0	61.8	47.6	54.8	48.0	31.0	24.0	112.0	2.0	0	46.0	52.0	42.0

$\bar{d}$, μm	Local time, h										Average	Volcancito	
	15	16	17	18	19	20	21	22	23	24		12	13
12.5	3.53	4.84	2.21	1.32	1.76	0.880	0.767	1.54	2.51	1.54	1.47	1.45	2.42
8.5	2.71	2.22	2.22	1.60	0.814	0.863	0.740	1.11	1.31	1.36	1.23	3.21	13.4
5.5	3.37	2.20	3.74	3.34	2.25	1.58	1.76	1.91	1.41	1.91	1.86	5.04	7.33
3.0	4.58	7.48	5.28	3.85	3.23	2.38	2.20	1.89	2.88	2.66	2.60	4.07	6.38
1.75	1.94	0.840	0.660	0.780	1.14	1.14	1.04	0.960	1.08	1.26	0.996	4.56	2.40
1.25	1.08	2.29	1.28	0.968	1.05	0.880	0.770	0.836	0.880	0.814	0.954	1.54	0.44
0.95	1.47	2.39	1.29	1.71	1.47	2.21	1.47	1.65	1.75	1.88	1.84	2.30	6.72
0.85	6.15	2.95	2.43	2.08	2.95	2.75	4.80	4.67	4.80	3.81	4.99	12.5	5.25
0.75	83.6	9.24	4.53	2.53	7.35	8.36	12.8	1.72	22.4	18.0	16.8	27.7	15.4
0.65	72.3	17.1	13.2	13.2	22.8	20.1	44.4	43.8	42.6	40.2	42.9	94.5	27.6
0.55	43.4	52.6	31.2	47.7	49.3	29.0	79.2	75.6	73.8	69.9	55.3	69.3	64.2
0.47	28.0	74.6	80.0	74.0	62.6	70.3	35	46.0	53.6	52.0	50.7	14.0	65.0

Figure 10 presents average volume particle size distribution functions for different time of a day. The well-defined diurnal evolution of particle size spectrum is observed: three modes of particle size distribution coexist and simultaneously change as functions of near-ground wind velocity and soil and air temperatures. In the afternoon, the strong minimum for the particles with size from 0.9 to 2 μm disappears due to the same factors. At nighttime hours, the maximum disappears for particles with $d > 7$ μm.

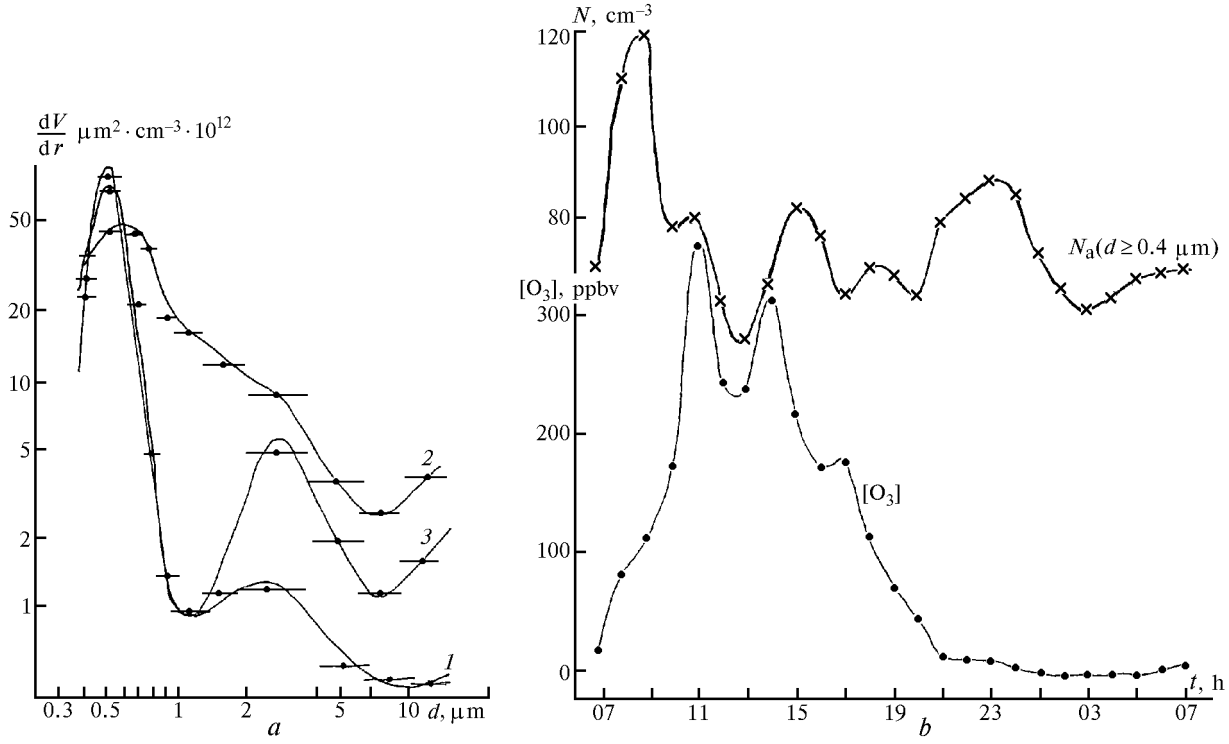

FIG. 10. Average size distributions of the volume aerosol density for different times of a day: 07:00–09:00 LT (1), 10:00–12:00 LT (2), and 14:00–15:00 LT (3); as well as diurnal behaviors of number density N_a of aerosol particles with $d > 0.4$ μm and ozone concentration $[O_3]$ in ppbv on May 9–11, 1995, at Playon.

The turbulent exchange and convective motions of air masses are time varying processes, and their modulating effect is clearly seen in the diurnal behaviors of aerosol and ozone concentrations (Fig. 10*b*). Evidently, these processes cause minima in N_a and $[O_3]$ concentrations at 12:00–13:00 and 15:30–17:00 LT, whereas particle sedimentation in absence of turbulence is responsible for N_a maximum at 23:00 LT. From radiation measurements at rancho Refuhio, as part of the experiment, we determined a marked increase of aerosol concentration in the entire atmospheric depth. The residual aerosol optical depth τ_a varied from 1 on May 9 to 1.8–2 on May 11. However, on May 9 at 14:00–15:00 LT, τ_a increased to 3.5–4.0, probably due to the strongest volcanic emission on that same day.

The results of multielement analysis of aerosol samples and dry deposit on the polyethylene film are presented in Table IX. It follows from these data that the highest aerosol concentration due to volcanic eruption occurred on May 9, precisely when the τ_a maximum was observed at rancho Refuhio in afternoon hours. Interestingly, sampled aerosol particles were larger than that on subsequent days and mostly contained terrogenic species Si, Al, Ca, Fe, and K. During night between May 10 and 11, sulfur-bearing particles rapidly increased in concentration most probably due to conversion of sulfur gas into aerosols; this is consistent with observed increase in residual optical depth τ_a on May 11–12.

TABLE IX. Results of multielement analysis of aerosol samples and dry deposit acquired in the region of Playon on May 9–11, 1995.

Species	Aerosol samples, ng/m³			Deposit, ng/m²	
	9.05 10.00–19.00	9–10.05 20.00–6.30	10–11.05 19.00–7.15		
Al	1660	< 800	< 700	1400+	/–400
Si	44300	3500	5900	34800	800
P	< 300	210	< 200	< 400	
S	3040	7190	11220	1400	300
Cl	550	< 200	< 100	< 200	
K	260	< 60	50	530	20
Ca	1020	150	150	2200	400
Ti	119	11	8	230	50
Cr	21	20	12	40	16
Mn	44	20	19	104	16
Fe	985	50	93	3000	300
Ni	4.3	1.2	2	14	5
Cu	< 10	< 10	6.4	8	6
Zn	< 2	12.3	< 2	67	6
Ga	< 1	< 1	< 1	4	2
Se	3.2	0.6	0.6	9	2
Br	5.8	5	4.9	6	3
Rb	3.1	3.7	5.9	10	4
Sr	20	7	4	72	5
Zr	12	11	18	22	6
Hg	–	6	3	–	
Pb	1.1	0.3	< 5	< 40	
Th	8	14	16	–	

4.3.2. Observations at rancho Refuhio

Measurements of aerosol and radiative characteristics, as well as near-ground ozone concentration were performed on three days: May 17, 18, and 19. Variations of the mean $\Delta N_a(d_i - d_{i-1})$ (in cm^{-3}) and $[O_3]$ (in $\mu g/m^3$) values during this time period are presented in Table X. As seen, midday variations of N_a and $[O_3]$ here are not so clearly correlated as in Playon region, probably due to the strong influence of advection of air masses on these characteristics. It should be noted that overnight the ozone concentration substantially decreases to small, but nonzero values (Fig. 11).

Aerosol concentration in the region of rancho Refuhio is much lower than in Colima-city, while variations of particle concentration are less pronounced than in Playon region. The diurnal behavior of particle size spectrum has a regular character, attributable to the processes of air mass circulation; however it may be occasionally distorted by irregular volcanic emissions.

The similar situation takes place for the residual atmospheric optical depth. In most cases, τ_a is practically constant during a day and slightly increases in the afternoon; but sometimes it may suddenly change. For instance, on May 17–19, increased atmospheric turbidity was observed. The optical depth τ_a exceeded unity almost all the time; and atmospheric turbidity rapidly increased on May 19, as early as at 07:00 LT. It should be noted that this agrees reasonably well with the data of photoelectric counter and the results of multielement analysis of aerosol samples (Table XI). Compared with Colima-city, the concentrations of most species here are substantially lower, except for Hg, Cr, Ni, Th, and Se species, whose increased concentrations are probably due to specific features of their emission to the atmosphere and specific evolution of particles containing them.

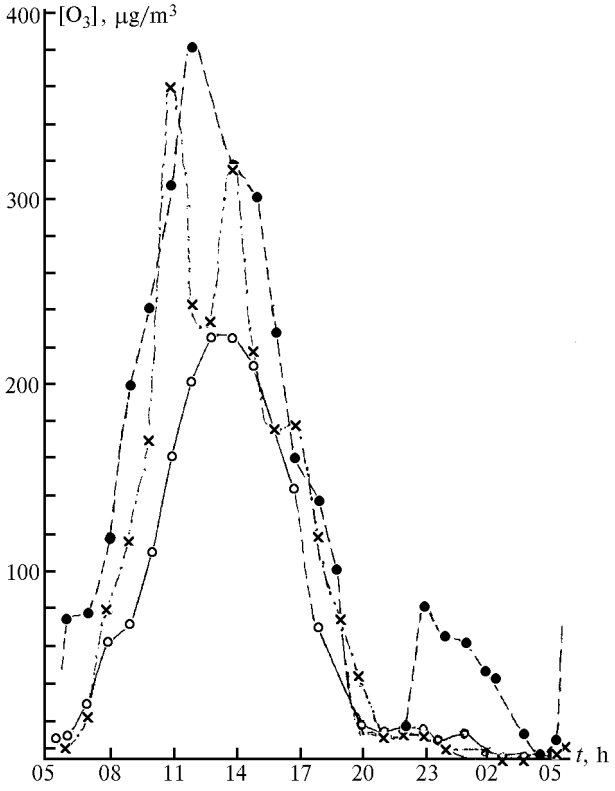

FIG. 11. Average diurnal behavior of near-ground ozone concentration in May of 1995 at three locations: the University Center (closed circles, dashed line), rancho Refuhio (open circles, solid line), and Playon (crosses, dot-and-dash line).

TABLE X. Diurnal behavior of particle number density $\Delta N_a(d_i - d_{i-1})$ (in 1/liter) and ozone concentration $[O_3]$ (in $\mu g/m^3$) at rancho Refuhio in May of 1995.

Δd, μm	Local time, h											
	01	02	03	04	05	06	07	08	09	10	11	12
> 10	3	1.5	1.5	1	1.7	1.5	8	8.5	8	10	9	10
10–7	1	3.5	4.5	4.8	2	3	14	17	14	13	22	8
7–4	6	9	4	1.2	15	8	3	33.5	28	30	95	32
4–2	32	34	28	26	44	70.5	85	100	188	187	225	190
2–1.5	12	27	16	34	54	39	74	90	71	84	88	110
1.5–1.0	30	24	41	113	180	126	300	176	177	167	212	254
1.0–0.9	50	116	38	50	113	212	636	515	100	323	443	172
0.9–0.8	90	485	917	570	190	1240	1500	1000	294	220	575	567
0.8–0.7	1530	4100	7650	4600	1800	10100	10080	4360	670	1170	2000	1030
0.7–0.6	10050	10400	10200	8800	6500	10600	8000	17200	2950	3200	5480	2940
0.6–0.5	32000	28400	24200	25900	29800	22100	24500	30000	15300	22500	18400	22000
0.5–0.4	20600	19500	18700	24500	30200	18100	43000	29200	41300	44700	42400	48400
Σ	64400	63100	61800	64600	68900	62500	88200	81700	61100	72600	69600	75700
O_3	8	8	7	5	8	15	28	58	92	115	174	176

Δd, μm	Local time, h											
	13	14	15	16	17	18	19	20	21	22	23	24
> 10	9	11	13	9	8	8	10	17	4	1.8	1.2	2
10–7	11	16	15	16	15	12	4	0	1	1	0.4	1
7–4	48	62	61	66	69	52	38	38	29	9.2	7.4	7
4–2	109	115	129	137	106	132	76	62	34	27	25	28
2–1.5	151	103	117	104	76	103	92	108	20	18	35	23
1.5–1.0	163	172	78	194	141	130	175	92	68	50	46	38
1.0–0.9	97	173	253	106	119	48	165	383	37	85	80	65
0.9–0.8	312	310	240	131	180	134	695	750	232	1110	2170	616
0.8–0.7	830	1050	560	777	320	556	2380	2260	1340	3700	5820	2870
0.7–0.6	2870	3750	3700	3100	3410	1255	10065	19590	14485	12700	10500	10150
0.6–0.5	21200	19400	15300	17860	16630	8220	24300	20750	17900	20300	23000	27500
0.5–0.4	35800	42700	47600	44600	40900	38650	27700	29850	39350	19800	14500	19500
Σ	61600	67800	68200	67100	62000	49300	65700	73900	73500	57900	58100	60800
O_3	194	211	200	169	131	92	44	38	22	20	18	11

TABLE XI. Chemical composition of aerosol samples at rancho Refuhio.

Species	Concentration, ng/m^3					Error, %
	23.12.94 10–14	17.05.95 10.30–19	17–18.05 19–7.30	18–19.05 16–9	19.05 9–16	
Al	10200	2330	610	1120	2620	15
Si	28000	18400	6050	5300	26800	3
P	3400	310	210	340	< 400	50
S	44000	5000	2660	2190	7760	20
Cl	3970	< 200	240	110	< 200	5
K	< 200	160	110	150	205	6
Ca	610	470	170	490	610	2
Ti	36	44	44	63	161	8
Cr	34	10	11	24	30	25
Mn	12	25	6	7	53	20
Fe	300	316	108	124	113	2
Ni	20	7.6	3.2	2.5	9	20
Cu	86	15.6	< 9	< 6	< 20	10
Zn	24	4.1	1.1	1.3	< 4	7
Ga	4	3	3	2	2	40
Se	10	1.4	2.1	4.6	4.6	40
Br	< 6	2.1	1.2	1.2	4.6	25
Rb	17	8	6.6	6.6	9.4	30
Sr	9	12	17	11	22	25
Zr	17	18	17	13	20	30
W	29	13	12	9	18	40
Hg	24	6	6	6	10	15
Pb	34	18	19	35	21	10
Th	< 5	9	12	7	22	20

4.3.3. Measurements at the University Center for Atmospheric Studies

At the University Center for Atmospheric Studies, the meteorological atmospheric characteristics are observed from automatic meteorological station operating since the late 1993. Aerosol measurements were initiated in December 1994, while measurements of ozone and sulfur gas have been regular since May 1995. These measurements were made just after those at rancho Refuhio between May 19 and 21, and later in June.

It should be noted that the meteorological conditions changed insignificantly during May; so the averaged data from all the three observations can be regarded quite representative of this period characterized by dry fair weather and absence of intense regular air motions in the near-ground atmospheric layer and the troposphere. Fuego de Colima volcano emitted little amount of aerosols and gases, at least an order of magnitude less than that in December. At the same time, the lack of developed cloudiness and precipitation has led to aerosol accumulation in the atmosphere. Data on aerosol concentration and dispersion are given in Table IV, and the data on aerosol chemical composition are presented in Tables V and VI; they can be considered representative not only as averages over period April through June, but also as characteristic of the time period when the experiment was performed at all measurement sites.

5. CONCLUSION

A series of measurements of some atmospheric parameters was performed in dry season in the vicinity of Fuego de Colima volcano; despite the general conditions in the lower atmospheric layers were quite stable during the measurements, they revealed a substantial influence of this volcano and its gas and aerosol emissions upon these parameters.

Most meteorological parameters exhibit distinct diurnal behavior determined by stable air mass circulation in the vicinity of the volcano.

In the lower atmospheric layers, accumulation of atmospheric pollutants, primarily sulfur gas and aerosols, takes place.

In dry season, the troposphere scavenged quite weakly. The instrumented observations in the

atmosphere has revealed weakly blurring jets of a substance, attenuating short-wave solar radiation.

As actinometric measurements indicate, the atmospheric optical depth strongly varies from $\tau_a < 0.1$ to $\tau_a = 1.5–5.0$ in the UV spectral range.

Very high concentrations of ozone, sulfur gas, and aerosol were observed in the near-ground atmospheric layer.

Aerosol measurements have revealed three maxima in the diurnal behavior of aerosol concentration: morning maximum between 06:00 and 08:00 LT for particles with $d \geq 0.7$ μm; midday maximum between 11:00 and 15:00 LT for particles with $d \geq 1.0$ μm; and evening maximum between 21:00 and 23:00 LT for particles with $10 > d > 2.0$ μm and $d < 0.7$ μm.

Multielement analysis of samples has shown that the species exhibit selective character of particle size distribution functions, and, perhaps, there are several sources of aerosol substance; but the Fuego de Colima volcano is the major aerosol source in the near-ground atmospheric layer, much more important than surface soil dusting and traffic exhausts.

Based on the results of numerous aerosol measurements, it can be stated that the particle size spectrum of volcanic aerosols has specific features, such as markedly higher concentration of particles in the size ranges $0.7 \leq d \leq 1.0$ μm and $2.0 \leq d \leq 4.0$ μm than those in the model spectra for global background, continental, and soil aerosols.

After the eruption of Popocatepetl volcano, the emitted species became dominating in the troposphere over Mexico, even in its eastern part. This fact is supported, particularly, by the similarity of chemical composition and dispersion properties of aerosol particles in the regions of Fuego de Colima and Popocatepetl volcanoes.[12]

REFERENCES

1. K.Ya. Kondrat'ev, ed., *Aerosol and Climate* (Gidrometeoizdat, Leningrad, 1991), 541 pp.
2. S.S. Khmelevtsov, ed., *Volcanoes, Stratospheric Aerosol, and Climate on the Earth* (Gidrometeoizdat, Leningrad, 1986), 256 pp.
3. L.S. Ivlev, J. Galindo, and V.I. Kudryashov, in: *Volcan Popocatepetl estudias reabilizados durante la crisis de 1994–1995*, Con. Cient. Asesor CENARDED-UNAM (1995), pp. 257–284.
4. J.B. Pollack and T.P. Ackerman, Geophys. Res. Lett. **10**, No. 11, 1057–1060 (1983).
5. V.D. Burlakov, F.B. El'nikov, V.V. Zuev, et al., Atmos. Oceanic Opt. **6**, No. 10, 701–706 (1993).
6. *Manual on Actinometric Observations at Hydrometeorological Stations* (Gidrometeoizdat, Leningrad, 1971), 223 pp.
7. T.B. Evnevich and L.N. Savinova, Meteorol. Gidrol., 106–109 (1989).
8. L.S. Ivlev, V.M. Zhukov, V.I. Kudryashov, and E.F. Mikhailov, Atmos. Oceanic Opt. **6**, No. 10, 715–726 (1993).
9. V.I. Kudryashov, S.F. Gundorina, and M.V. Frontas'eva, "*Chemical composition of filters used for atmospheric air sampling*", (Report No. 18-91-443, Dubna, 1991), 20 pp.
10. V.P. Chelibanov, ed., *Analytical Devices for Ecological Applications*. Catalogue (St. Petersburg, 1994), 78 pp.
11. L.S. Ivlev, in: *Abstracts of Reports at the Workshop on Aerosols of Siberia*, Institute of Atmospheric Optics SB RAS, Tomsk (1995), p. 20.
12. L.S. Ivlev, A.O. Vargas, E.A. Chavez, et al., in: Proceedings of the Geophys. Congress (Mexico, October, 19, 1995, Valrata), pp. 23–25.